

## Altered Behavior, Physiology, and Metabolism in Fish Exposed to Polystyrene Nanoparticles

Karin Mattsson,<sup>\*,†</sup> Mikael T. Ekvall,<sup>‡</sup> Lars-Anders Hansson,<sup>‡</sup> Sara Linse,<sup>†</sup> Anders Malmendal,<sup>§</sup> and Tommy Cedervall<sup>†</sup>

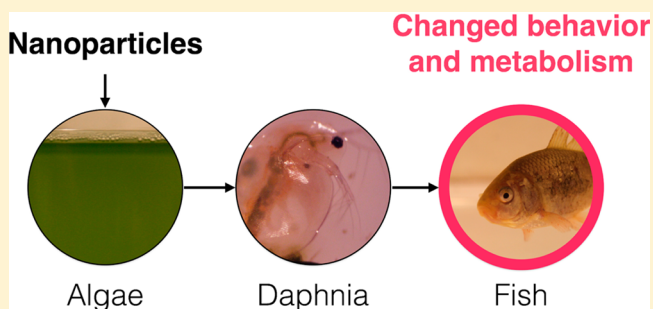
<sup>†</sup>Department of Biochemistry and Structural Biology, Lund University, P.O. Box 124, SE-221 00 Lund, Sweden

<sup>‡</sup>Biology/Aquatic Ecology, Lund University, SE-223 62 Lund, Sweden

<sup>§</sup>Department of Biomedical Science, University of Copenhagen, Blegdamsvej 3, DK-2200 Copenhagen, Denmark

### S Supporting Information

**ABSTRACT:** The use of nanoparticles in consumer products, for example, cosmetics, sunscreens, and electrical devices, has increased tremendously over the past decade despite insufficient knowledge about their effects on human health and ecosystem function. Moreover, the amount of plastic waste products that enter natural ecosystems, such as oceans and lakes, is increasing, and degradation of the disposed plastics produces smaller particles toward the nano scale. Therefore, it is of utmost importance to gain knowledge about how plastic nanoparticles enter and affect living organisms. Here we have administered 24 and 27 nm polystyrene nanoparticles to fish through an aquatic food chain, from algae through *Daphnia*, and studied the effects on behavior and metabolism. We found severe effects on feeding and shoaling behavior as well as metabolism of the fish; hence, we conclude that polystyrene nanoparticles have severe effects on both behavior and metabolism in fish and that commonly used nanosized particles may have considerable effects on natural systems and ecosystem services derived from them.



### INTRODUCTION

The production of polymeric plastic products has increased since the 1960s, and 280 million metric tonnes were produced globally in 2012.<sup>1</sup> Less than half of this mass was consigned to landfill or recycled.<sup>1</sup> When plastic is released into the environment, a noticeable amount will end up in the aquatic environment. The estimated amount of plastic in the open-ocean surface is between 7,000 and 35,000 metric tonnes,<sup>2</sup> and plastic in the ocean is degraded into smaller pieces through UV-radiation, mechanical abrasion, biological degradation, and disintegration.<sup>3,4</sup> These pieces may have harmful effects on aquatic organisms when degraded.<sup>5</sup> Large items will cause entanglement, impaired feeding, and mortality to birds, turtles, and mammals.<sup>6</sup> Our limited knowledge of the effects of smaller items, observed at micrometer or less,<sup>7</sup> is alarming as the amounts of plastics in lakes, oceans, and plankton have increased over time since the 1960s,<sup>7</sup> and the discharge will likely accelerate in the future.

Engineered nanoparticles will end up in soil or water, such as oceans and lakes, through sewage plants, waste handling, or aerial deposition even if they are released into the atmosphere<sup>8</sup> or disposed in landfills.<sup>9</sup> The mobility, biological fate, and bioavailability depend on size, shape, charge, and other nanoparticle properties.<sup>10,11</sup> Aggregation modulates the concentration of single nanoparticles in a complex manner. Living organisms can be exposed to nanoparticles directly or

indirectly, for example, through plants,<sup>8</sup> which may act as an entry route for nanoparticles into food chains.<sup>9</sup> This has been found for gold nanorods.<sup>12</sup> The most likely uptake route of terrestrial organisms is through inhalation or ingestion, whereas direct passage across gills or external surface epithelia are most likely important routes for aquatic organisms.<sup>13,14</sup> The common crustacean zooplankton, *Daphnia magna*, can ingest particles in the size range of 20–70  $\mu\text{m}$ <sup>15</sup> and is therefore a likely entry point for nanoparticles into aquatic food webs. Natural nanoparticles with at least one dimension in the size range of 1–100 nm exist in aquatic systems, from subsurface aquifers to lakes and rivers,<sup>16</sup> and the concentrations of, for example, nanosized  $\text{TiO}_2$  particles in surface waters have been estimated to 21 ng/L and for sewage treatment effluents 4000 ng/L.<sup>17</sup>

When nanoparticles are released into the environment, they will interact with the surrounding materials. In lakes, there will be organic breakdown products,<sup>18</sup> and once the nanoparticles enter an organism, they will encounter very complex biological fluids. Proteins and other biomolecules will bind to the nanoparticle surface, creating a corona.<sup>18,19</sup> The composition of the corona will change over time depending on the

Received: July 23, 2014

Revised: November 6, 2014

Accepted: November 7, 2014

Published: November 7, 2014

composition of the surrounding biological fluid and on the exchange rates and affinity to the nanoparticle surface.<sup>20,21</sup> The formation of the corona will be even more complex when the nanoparticle travels between compartments or organisms.<sup>22,23</sup> The corona governs the interactions of a nanoparticle with biological systems. Polymeric plastic nanoparticles interact with many proteins important for fat metabolism, immune defense, and blood coagulation.<sup>22,24</sup> One example is the HDL, which transports lipids, such as triglycerides and cholesterol, in blood and cells.<sup>25</sup> The major apolipoprotein in HDL is ApoA-I, and this, as well as other apolipoproteins, is found in most of the studied coronas around nanoparticles,<sup>26,27</sup> including polystyrene nanoparticles in fish blood.<sup>25</sup> Intact HDL has been found to bind to copolymer nanoparticle surfaces.<sup>26</sup> This is a worrisome finding because the energy metabolism in fish is more based on fat metabolism than in mammals,<sup>28</sup> and it has previously been shown that polystyrene nanoparticles disturb the fat metabolism in fish.<sup>25</sup>

The present study focuses on effects in behavior and metabolism of nanoparticles in an aquatic ecosystem. Polystyrene nanoparticles were selected since they are one of the five main types of produced plastic<sup>29</sup> and are commonly found in aquatic environments.<sup>30</sup> Since a considerable amount of the nanoparticles used is transported into aquatic ecosystems through the sewage system and, in addition, a large amount of all plastic products is broken down to small particles in lakes and oceans, we have used an aquatic food chain as a model system. The aim of our study was to investigate if and how these nanosized particles, transported through the food chain, affect the metabolism and behavior of the top consumer, fish. We have used statistical analyses of video-recorded feeding sessions to study differences in activity and shoal behavior between control and nanoparticle-fed fish. Information on changes in metabolite levels gives an insight into the condition of an organ.<sup>31</sup> NMR spectroscopy has been used to study metabolic differences in separate organs, while weighing and measuring were used to evaluate any gross growth effects.

## MATERIALS AND METHODS

**Nanoparticles.** Sulfonated polystyrene nanoparticles, 24 and 27 nm (Bang laboratories, Fisher, IN, USA), were used in the study. The particles were dialyzed against copper-free tap water during 3 days, and the water was exchanged every day. The size of the particles was confirmed with measurements by DLS using a Malvern Zeta NANO S (Malvern Instruments Limited, UK) and by NTA using a NanoSight LM10 (Nanosight Ltd., Amesbury, UK). The particles were measured after they were dialyzed; the 24 nm particles monitored with DLS were  $24.7 \pm 0.2$  nm (fwhm 35 nm), and the 27 nm monitored with NTA were 27.5 nm (fwhm 15 nm). The two batches of particles have almost the same size distribution before and after dialysis, and they were therefore used as equivalent particles in this study. The particles were stabilized by the surface modification, that is, the sulfonate groups. No other stabilizing chemical was added. The concentration of the nanoparticles given to the algae was 0.01% (w/v) or  $9.3 \times 10^{12}$  particles/mL, which corresponds to a total surface area of approximately 4 m<sup>2</sup>, assuming that the particles are solid spheres. The number of nanoparticles reaching each fish was calculated to be approximately  $1 \times 10^{13}$  particles (130 mg particles per feeding), assuming that the algae were covered with particles and that *Daphnia* consumed 60% of the given algae during 24 h of feeding. The transfer of nanoparticles from

algae to *Daphnia* was previously verified using fluorescent polystyrene particles.<sup>25</sup>

**Algae (*Scenedesmus sp.*).** Algae with an approximate size of 25  $\mu$ m diameter were cultivated in six 1 L bottles. The relation between the total algal volume and the particle concentration remained constant during the experiment, but the volume and the concentration of the algae varied. On day 31 of the experiment, the concentration of algae presented to zooplankton was increased to optimize the exposure to nanoparticles and speed up the effects on the fish. However, the volume of the algae and the amount of nanoparticles were the same as in the beginning of the experiment.

**Zooplankton (*Daphnia magna*).** The zooplankton species *Daphnia magna*, which was used in the study, originated from Lake Bysjön (55° 40' 31.3" N, 13° 32' 41.9" E) but have been kept under controlled laboratory conditions for more than 100 generations. The animals were fed twice a week with an algal culture dominated by the green algae, *Scenedesmus sp.*

**Crucian Carp (*Carassius carassius*).** Crucian carp were collected from Lake Trollsjön in Eslöv, southern Sweden (55°50'15.3" N, 13°17'16.4" E) on day -8, that is, eight days before the start of the experiment. On day -2, four fish were put into each aquarium (total number of aquaria was 12), and they were measured (8.2–9.6 cm), weighed (7.5–13.7 g), and their fins were marked in order to distinguish between individuals. The experiment started on day zero, when one fish from each aquarium was removed and euthanized in order to obtain starting values for the metabolism. The *Daphnia* were fed to the remaining fish (20 *Daphnia*/fish, that is, 60 zooplankton per aquaria) in the aquaria, and the feeding time (defined as the time to consume 92–95% of the *Daphnia*) as well as the number of ingested *Daphnia* for each fish was measured.

**Food Chain.** The food chain consisted of three trophic levels, including algae (*Scenedesmus sp.*), zooplankton (*Daphnia magna*), and crucian carp (*Carassius carassius*). The experiment was designed as a three-day cycle with two parallel chains, one chain receiving nanoparticles in tap water (treatment) and the other tap water only (control). On day one, dialyzed polystyrene particles (or water) were added to algae. The bottles were shaken for 2 min, and the algae were grown for 24h. On day two, adult *Daphnia* with an approximate size of 3 mm were collected and allowed to feed on the algae during 24h. The *Daphnia* showed no changes in behavior after 24h of ingestion of algae. On day three, the *Daphnia* were collected on a net with a mesh size of 50  $\mu$ m and washed two times with 250 mL of water to reduce free nanoparticles before they were fed to the fish. Every step in the chain had a day–night cycle of 12 h–12 h, and the temperature was 19 °C.

**Ethical Permission To Perform the Study.** The study was granted ethical permission from Malmö/Lund Ethical committee (D nr 14 13–12) and was performed according to the current laws in Sweden.

**Aquaria and Water.** Plastic aquaria with a size of 18 L were filled with 15 L of copper-free water. Copper-free water was used during the whole experiment. All water contaminated with nanoparticles was collected and sent for destruction after the experiment was finished.

**Behavior.** The behavior of the fish was monitored by filming during feeding on day zero, day 24, and day 61. Each aquarium was moved to a location that was set up for filming the fish. All aquaria were placed in the same position with equal distance to the camera, and aquaria walls were covered on three

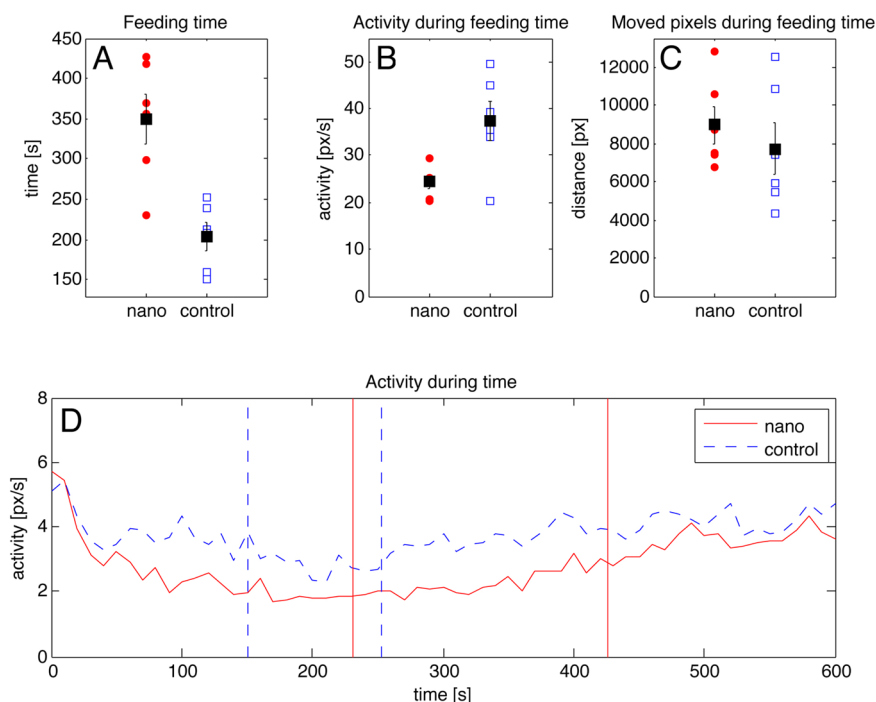


**Figure 1.** Fish activity. Nanoparticle-fed fish are marked as red dots ( $N = 6$ ), and control fish are marked as blue squares ( $N = 6$ ) for each aquaria. Black squares represent the mean overall aquaria in each group, and error bars represent the mean standard deviation. (A) Feeding time in seconds, that is, the time it takes for the fish to eat 92–95% of the food in each aquarium. (B) Mean activity for the fish in each aquarium during feeding time displayed as moved pixels/second. (C) Moved distance in pixels during feeding time for each aquarium. (D) Mean activity for the fish during 10 min. Nanoparticle-fed fish are marked in solid red ( $N = 61$ ), and control fish are marked in dotted blue ( $N = 61$ ); the activity is displayed as pixel/second. Vertical lines represent the shortest and longest feeding time for nanoparticle-fed fish (solid red) and control fish (dotted blue), respectively.

sides with white paper to reduce reflection. The fish were allowed to acclimatize for 30 min before they were filmed during 30 min. The movies were cut so that the starting time for each movie was when the *Daphnia* entered the aquarium. These movies were then analyzed using the software ImageJ (free available software). Each aquarium was analyzed for 10 min. From the software, we got the position in pixels every second for each fish. These positional data were further analyzed using MATLAB to obtain activity, moved pixels, distance between fish, and the fish exploration of the aquarium.

**Organ Sampling and Analysis.** All fish were collected, and samples of skin mucus were taken before they were anaesthetized using benzocaine. They were measured and weighed before a blood sample was taken from the dorsal aorta. The blood was allowed to coagulate and was then centrifuged at 13 000 rpm using a table-top centrifuge (Microcentrifuge VWR 1814, from VWR International U.S.A.) at 14 kG, and the supernatant was collected and centrifuged at 13 000 rpm at 14 kG to remove cells and aggregates. The fish neck was cut, and the brain was collected. The abdomen was opened, and the heart, liver, and the bile were sampled. The fish scales were removed, and a sample of their muscle was collected in the dorsal part of the fish, close to the anterior dorsal fin. The gills were collected. All samples were stored at  $-80\text{ }^{\circ}\text{C}$ .

When the organs were collected, it was noticed that the muscles and the brain differed in texture and color between the two groups. The brain was therefore weighed, before and after being freeze-dried, to measure the difference in water volume.

**Preparations of Samples and  $^1\text{H}$  NMR Analysis.** Fish organs, including blood, gills, muscle, liver, and brain, were analyzed using NMR spectroscopy. The blood was dissolved in a 50 mM sodium phosphate buffer in  $\text{D}_2\text{O}$  at pH 7.4. Gills,

muscles, liver, and brain samples were freeze-dried and homogenized in the same buffer. From each of the samples, 650  $\mu\text{L}$  were transferred into a 5 mm NMR tube. The NMR measurements were performed at  $25\text{ }^{\circ}\text{C}$  using a Bruker Avance-III 600 spectrometer (Bruker Biospin, Rheinstetten, Germany) operating at a  $^1\text{H}$  frequency of 600.13 MHz and equipped with a double-tuned  $^1\text{H}$ – $^{13}\text{C}$  cryoprobe. The  $^1\text{H}$  NMR spectra were obtained through a single- $90^{\circ}$ -pulse experiment. Signals from high-molecular-weight components were decreased by adding a CPMG delay of 40 ms, with a spin-echo delay of 200  $\mu\text{s}$ . During the relaxation delay of 4 s, the water signal was suppressed by a presaturation pulse. The resulting spectra were collected over 64 transients and had a total of 98 304 data points spanning a spectral width of 24 ppm. During these procedures, one of the gill and liver, three of the blood, and four of the muscle samples were spoiled or did not produce good NMR spectra and were excluded from further analysis. For assignment purposes, 2-dimensional  $^1\text{H}$ – $^1\text{H}$  COSY,  $^1\text{H}$ – $^1\text{H}$  TOCSY,  $^1\text{H}$ – $^{13}\text{C}$  HSQC, and  $^1\text{H}$ – $^{13}\text{C}$  HSQC-TOCSY spectra were acquired.

**NMR Metabolic Data Treatment.** The spectra were processed using the software iNMR ([www.inmr.net](http://www.inmr.net)). Prior to the Fourier transformation, an exponential line broadening of 0.5 Hz was applied to the free-induction decay. All of the spectra were manually phased and baseline corrected and referenced to the alanine methyl signal at 1.47 ppm. The region around the residual water signal was removed so as not to compromise the analysis. (The removed region varied between organs but typically comprised the region 5.0–4.6 ppm). The high- and low-field ends of the spectra, where the only signal came from the reference substances TSP, were also removed, which left the region between 9.5 and 0.5 ppm. For all organs

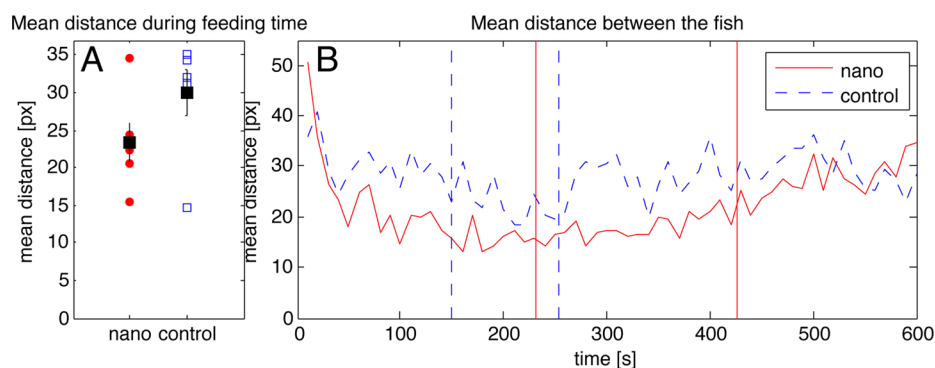


**Figure 2.** Distance between fish. (A) Mean distance in pixels between the fish during feeding time in each aquarium. Nanoparticle-fed fish are marked as red dots ( $N = 6$ ), control as blue squares ( $N = 6$ ). Black squares represent the mean over all aquaria in each group, and error bars represent the mean standard deviation. (B) Mean distance between the fish in pixels during 10 min. Nanofed fish are marked solid red ( $N = 60$ ), control are marked dotted blue ( $N = 60$ ). Vertical lines represent the shortest and longest feeding time for nanoparticle-fed fish (solid red) and control fish (dotted blue), respectively.

except blood, the signals were normalized to the biopsy weight so that the  $^1\text{H}$  signal intensities correspond to the actual  $^1\text{H}$  concentration; the blood integrals were normalized to total intensity.

For the initial screening of significant effects of the nanodiet in the different organs, data was reduced into 0.01 ppm bins over which data were integrated. The resulting  $\sim 800$  integrals were pareto scaled and centered and subjected to PCA. The number of principal components was determined by leave-one-out cross-validation. Significant changes in the metabolome were identified using MANOVA on all principal components. Sequential Bonferroni<sup>32</sup> correction for multiple testing was applied. All multivariate analysis was preformed using Simca 13.0 (Umetrics, Umeå, Sweden).

Liver and muscle spectra were further analyzed in order to identify significant metabolite effects. Here the spectra were aligned using icoshift<sup>33</sup> so that the spectra could be analyzed at high resolution ( $\sim 25\,000$  intensities).

O2PLS-DA<sup>34</sup> models separating nano and control fish were built. Significant outliers were identified by PCA and excluded when the models were built and then were reintroduced and tested. During model building, the 25 000 variables were iteratively reduced to 5000 and 1000 for liver and muscle samples, respectively, without a loss of prediction power. The models were evaluated by the number of misclassifications by cross validation and by use of test sets that were left out when the model was built. The loadings and the correlation coefficient ( $R$ ) between intensities at the individual frequencies and the predictive component were calculated. A cutoff value for  $R^2$  corresponding to  $P < 0.05$  with Bonferroni correction for an assumed number of 100 metabolites was calculated from the distribution of  $R^2$  values in 10 000 permuted data sets. The assignments were done based on chemical shifts only using earlier assignments and spectral databases.<sup>35,36</sup>

## RESULTS

Sulfonated polystyrene nanoparticles were fed to fish through an aquatic food chain through algae and zooplankton (see scheme TOC art). The behavior of the fish was observed before, during, and after feeding. Before the food was added to the aquarium, all fish had a low activity. The addition of zooplankton resulted in increased activity, and clear differences in activity and hunting behavior between control and nanoparticle-fed fish were visible (see below). When all the

fish had eaten, their activity slowly decreased until it reached almost the same level as before they were fed. The differences between the groups progressively increased throughout the experiment.

After 61 days, the feeding behavior was video recorded for 30 min, starting a few seconds before the food (*Daphnia*) entered the aquaria. The feeding time was almost twice as long for the nanoparticle-fed fish compared to the controls ( $p = 0.0043$ , Mann–Whitney–Wilcoxon test) (Figure 1A). During feeding, the control fish showed significantly ( $p = 0.0006$ , Mann–Whitney–Wilcoxon test) higher activity (Figure 1B) than the control fish, and they were actively searching for food. The nanoparticle-fed fish moved much more slowly and did not hunt as actively as did the control fish. Despite the significant differences in speed, the total distance the fish swam to eat all the food was similar for both groups (Figure 1C). When the food entered the aquarium, there was an increased activity in both the nano and control groups, which after only a few seconds decreased rapidly (Figure 1D). The drop in activity was, however, deeper for the nanoparticle-fed group than for the control group, which continued to have a high activity and searched for food (Figure 1D). This difference in activity remained throughout the feeding. When feeding was completed, the activity increased back to baseline for both groups (Figure 1D).

Analyses of the mean distance between the fish in each aquarium revealed other surprising behavioral differences. This distance was smaller for the nanoparticle-fed fish than for the control fish (Figure 2A), which suggests that the nanoparticle-fed fish behaved more as a group also during feeding and exhibited stronger shoaling behavior than did the control fish (Figure 2B). The addition of food to the aquarium resulted in increased distances between the fish in both groups. However, similar to what was observed with respect to activity, the distances between individuals decreased rapidly (Figure 2B). The decrease was more pronounced for the nanoparticle-fed fish, and the difference remained throughout the feeding occasion (Figure 2B). When all the food was consumed, the distances among the nanoparticle-fed fish increased (Figure 2B).

Another difference between nanoparticle-fed and the control fish was observed in their swimming pattern during feeding. The nanoparticle-fed fish occupied less space of the aquarium than did the control fish (Figure 3A,B). The control fish

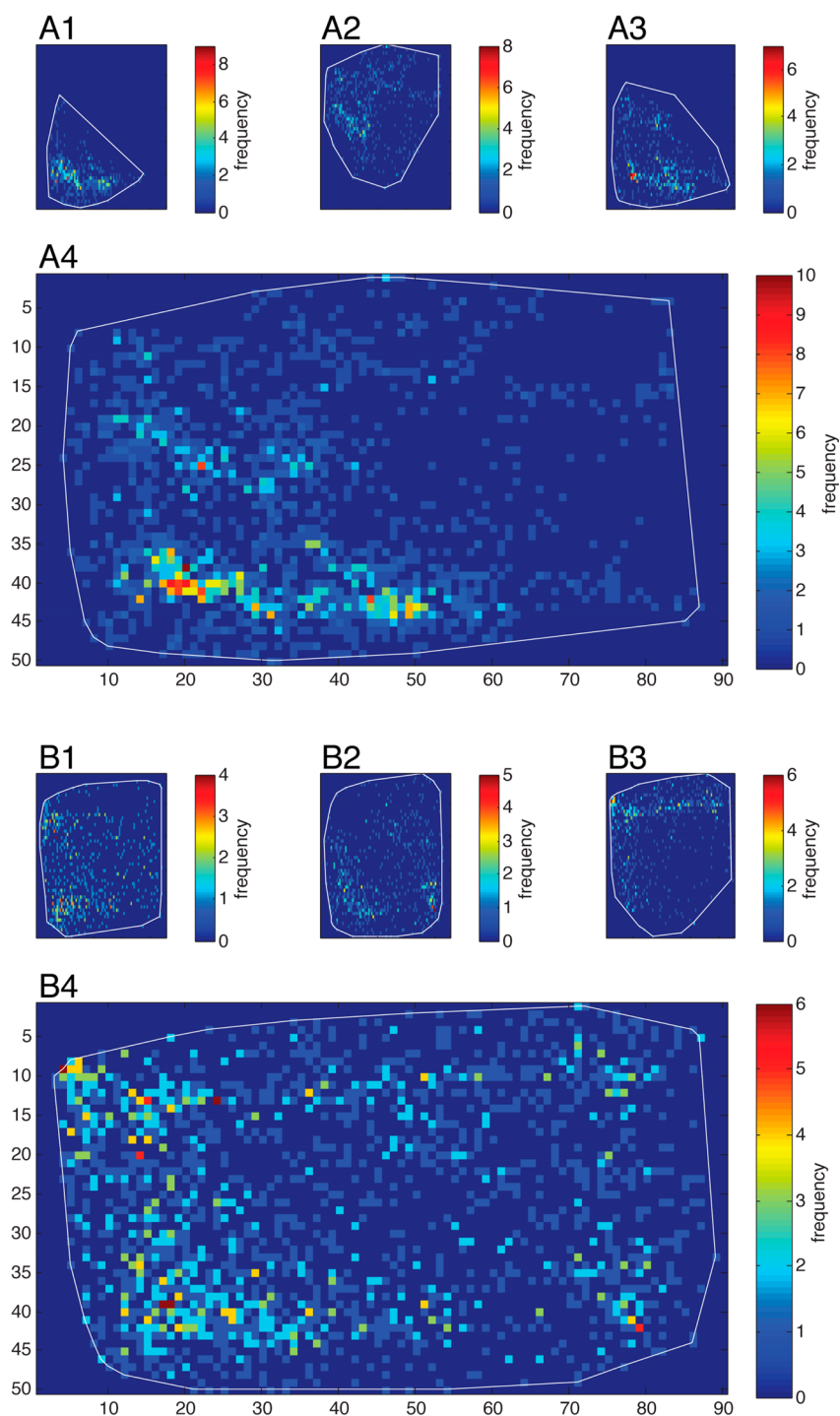


**Figure 3.** Position of each fish during 5 min in (A) a typical nanoparticle-group aquarium and (B) a typical control group aquarium for three individual fish (A1–3 and B1–3,  $N = 300/\text{figure}$ ) in one aquaria and the total movement for the three individual fish (A4 and B4,  $N = 900$ ).

actively explored almost the whole aquaria when searching and hunting for food, whereas the nanoparticle-fed fish explored lesser space ( $p = 0.0058$ , Mann–Whitney–Wilcoxon test).

The individual behavioral differences were greater among control fish than nanoparticle-fed fish, as illustrated by the larger variance when the activity versus the feeding rate per fish was plotted (Figure 4). To find if this is a general characteristic, we compared the variance for all parameters described here, and the variance was smaller for the nanoparticle-fed fish in four out of six analyses, (Figure S1, Supporting Information).

For example, for the activity during feeding, the variance between the groups indicates that one effect of the nanoparticles is a suppression of individual activity. The variation in metabolite concentration is generally of the same scale in the two groups. The one exception is found in the samples from gills, where the variation appears smaller in the nanoparticle-fed fish.

Fish organs, blood, brain, gills, liver, and muscle samples were analyzed by NMR spectroscopy to identify effects of the nanoparticle diet on the metabolite concentrations. Low-

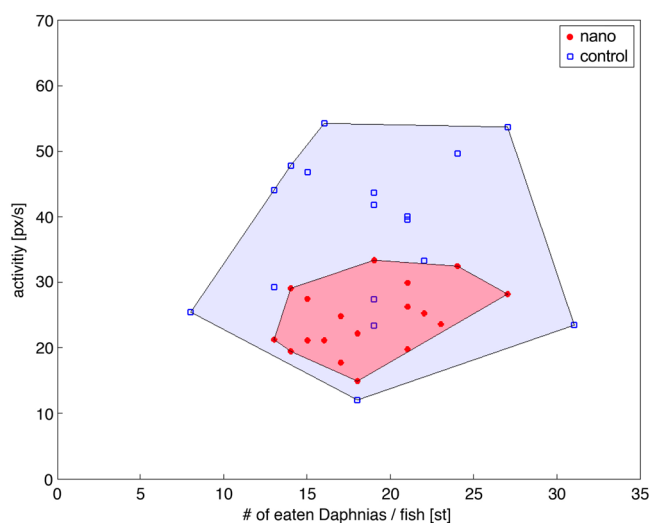


**Figure 4.** Activity versus feeding rate for each fish. Nanofed fish are marked as red dots ( $N = 18$ ), and control fish are marked as blue squares ( $N = 17$ ). Activity ( $y$ ) in pixels/second and numbers of eaten *Daphnia* during feeding time ( $x$ ) in numbers. The colored area contains the values in each group: nanogroup (light red) and control group (light blue).

resolution metabolite spectra were subjected to PCA. MANOVA was applied to identify organs with significant metabolite changes. There were significant differences in liver and muscle tissue (Table S1, Supporting Information). The separation between liver and muscle metabolomes of nanoparticle-fed fish and control fish is illustrated in Figure 5. It is important to note that there might be effects of the diet in the other organs that were not picked up by this procedure.

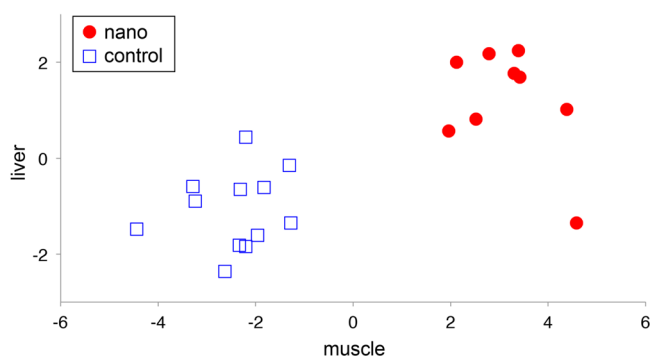


**Figure 5.** NMR metabolomics. The separation of the PCA scores for individual fish along the muscle ( $x$ ) and liver ( $y$ ) metabolite axes. The vectors were defined using MANOVA. Control fish are denoted with open blue squares ( $N = 11$ ), and nano fish are denoted with filled red circles ( $N = 8$ ).

To further characterize the metabolite changes induced in liver and muscle, we built OPLS-DA<sup>34</sup> models based on fully resolved NMR spectra. There are specific nano diet induced changes in the metabolite concentrations, increases in ethanol (1.17 ppm; Figure 6A) in the liver, and increases in inosine/adenosine (8.33, 6.09 ppm) and lysine (3.00, 1.89, 1.72, 1.50 ppm) in muscle (Figure 6B,C). If we remove the variation that is explained by the factors in the multivariate models that do not correlate with the nanoparticle diet, that is, that varied due to other factors than the presence of nanoparticles in the food, we can identify more metabolites that are affected by the diet.

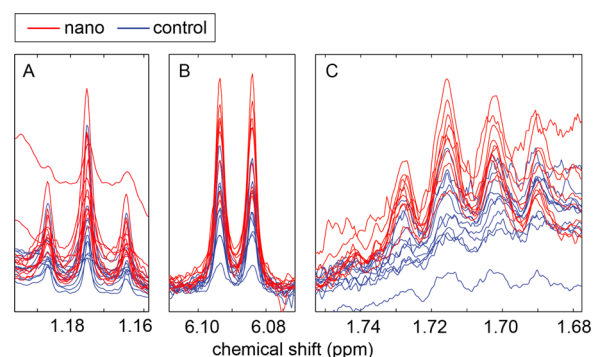


**Figure 6.** NMR spectra. Examples of spectra from liver (A,  $N = 24$ ) and muscle (B–C,  $N = 21$ ) samples. Panel A shows the ethanol signal in liver at 1.17 ppm. Panels B and C show the adenosine/inosine and lysine signals in muscle at 6.09 and 1.72 ppm, respectively. Spectra from control fish are shown in blue, and those from nano spectra are shown in red. The shown spectra are those used in the OPLS-DA models (Table S2, Supporting Information).

Increased concentrations of leucine (1.70, 0.94 ppm), phenylalanine (7.42, 7.37, 7.32 ppm), and tyrosine (7.19, 6.98 ppm) were detected in the liver, while ethanol was significantly lower in the muscles.

The correlations with the individual metabolites are weak, but there is a clear correlation at the metabolome level. It is thus the collective effects of many metabolite changes, rather than large changes in a few, that are responsible for the separation. To measure the predictive strength of the liver- and muscle-based OPLS-DA models, we took out random test sets consisting of three nano and three control samples, made new models, and used these to predict if the samples came from fish on a nanodiet or not. For the muscle samples, this worked very well, and all samples were correctly classified, which shows the strength of the separation (Table S2, Supporting Information).

The brain and the muscle differed between the groups both in texture and color. The brains in the nanoparticle-fed fish were much more fluffy, whiter, and appeared swollen. The brains of nanoparticle-fed fish were also significantly ( $p = 0.0067$ , Mann–Whitney–Wilcoxon test) heavier than were the brains of control fish (Figure 7A). They also contain significantly ( $p = 0.0016$ , Mann–Whitney–Wilcoxon test)

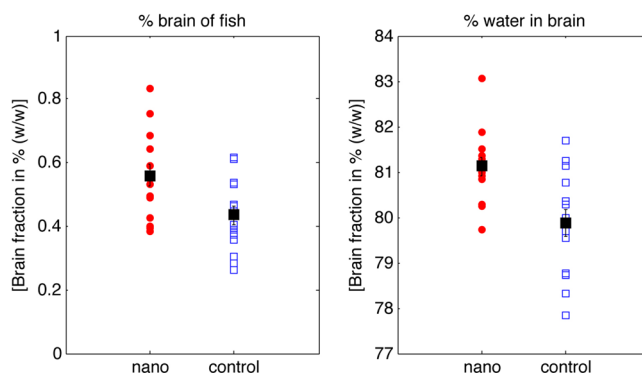


**Figure 7.** Brain status. The nanoparticle-fed fish are marked as red dots ( $N = 15$ ), and the control fish are marked as blue squares ( $N = 16$ ). Black squares represent the mean over all aquaria in each group, and error-bars represent the mean standard deviation. (A) Brain fraction in % (wet weight; w/w) of the total fish. (B) Water content in % (wet weight; w/w) of fish brain.

more water (Figure 7B), which possibly explains the fluffiness observed in brain from the nanoparticle-fed fish.

## DISCUSSION

Previous studies have shown that nanosized materials can affect the behavior of fish<sup>25,37</sup> and the function of their organs.<sup>37</sup> In our study, fish received nanoparticles through a natural three-trophic level food chain (algae, zooplankton, and fish) where fluorescent nanoparticles have been confirmed to be transported from the algae to zooplankton,<sup>25</sup> and we find considerable effects on fish behavior as a result of exposure to polystyrene nanoparticles through the food chain. The fish exposed to nanoparticles showed lower activity, increased feeding time, stayed closer together, and were less explorative. Furthermore, the results of NMR-based metabolomics show distinct differences in the metabolism between the nanogroup and control. The fact that it is the collective change of many metabolites rather than a few individual metabolites that separates the nanofed fish from the fish from the control group suggests a general disturbance of cellular function rather than specific effects due to the interaction of the nanoparticles with a distinct cellular process. Taken together, our results show that polystyrene nanoparticles induce considerable changes in metabolism and hunting behavior. In a broader context, a reduced feeding activity of fish will lead to reduced growth and ability to avoid predators and thereby reduce their fitness in natural ecosystems. Moreover, since fish have a strong impact and are key players in aquatic food webs, irrespective of food chain composition and climate conditions,<sup>38</sup> this will ultimately also lead to a reduced yield of fish biomass. Hence, nanoparticles entering lakes, rivers, and oceans through our sewage system may also negatively affect ecosystem services, such as fisheries, and thereby have considerable effects on human economic systems.

The fish were served a low amount of food to test the effects of nanoparticles when they needed to use their fat reserves. The similar activity and feeding rate in the beginning and the fact that all fish started to eat immediately indicate that all fish felt hunger and initially used stored and easily mobilized energy to gain more food. The more pronounced decrease in activity of the nanoparticle-fed fish suggests that their energy reserves were smaller or that the access to them was disturbed.

The nanoparticle-fed fish stayed closer to each other and did not explore the surroundings as much during feeding as the control fish. This indicates changes in hunting behavior and that the nanoparticle-fed fish show more shoaling behavior during feeding compared to control fish. This could be a result of metabolic changes but also of a direct effect on the brain. Fish exposed to nanoparticles in their environment can take up particles through their gills, and the particles can be transported to different organs, such as the brain.<sup>39</sup> We noted a difference in texture and color of muscles and brain, and the brains of the nanogroup contained more water than did the control brains, which suggests that the nanoparticles affected the texture of the brain tissue. Modulation studies suggest that polystyrene chains have strong affinity to lipids and affect the organization and function of biological membranes.<sup>40</sup> This likely explains how polystyrene can be trapped in lipid-rich organs, such as the brain, as well as the observed morphological changes in the brain. However, more knowledge of nanoparticle effects on metabolism in general and on the brain in particular is needed to explain the observed behavioral changes.

It took several weeks of feeding with nanoparticles (0.01% (w/v)) before a clear change in the behavior was observed. This indicates that the number of digested particles or the length of starvation are of importance. At least two explanations are possible. First, if the nanoparticles are accumulated in the fish, the amount of nanoparticles that influence the organism will increase over time. Second, the biological stress by the nanoparticles can for some time be compensated, but with time and starvation, the compensation collapses.

It has previously been shown that living organisms exposed to nanosized materials show biochemical changes in their organs.<sup>25</sup> Here we find a significant change in the metabolite profiles in at least two organs, liver and muscles. On the basis of the muscle metabolites we can build a model that successfully predicts if fish have been subjected to a nanoparticle diet. Although the predictive power of this particular model is likely limited to the controlled conditions explored here, one can envisage the use of a similar model to measure the level of nanotoxicity, to evaluate the exposure to plastic nanoparticles, or to nanoparticles of other materials at the individual level, both in laboratory settings and the natural habitat.

In conclusion, we show here that the uptake of nanoparticles through a food chain strongly affects behavior of top consumers by reducing their activity, feeding rate, and changing their social behavior. In addition, we demonstrate genetic changes in liver and muscle metabolism as well as morphological alterations in the brain and muscles. Our data thus suggests a linked response at the metabolic, morphological, and behavioral levels. The demonstrated behavioral changes in the top consumer will likely also have considerable effects at the ecosystem level. Hence, we conclude that the rapidly increasing use of polymeric nanoparticles as well as degradation of plastic material to nanosize cannot be ignored as a potent future environmental threat to the function of natural ecosystems as well as to ecosystem services, such as drinking water and fishing.

## ASSOCIATED CONTENT

### Supporting Information

Difference in coefficient of variance, ratio coefficient of variance/coefficient of variance for the control group and nanogroup; MANOVA of PCA scores based on signal intensities for different organs; and OPLS-DA model statistics. This material is available free of charge via the Internet at <http://pubs.acs.org>.

## AUTHOR INFORMATION

### Corresponding Author

\*E-mail: [karin.mattsson@biochemistry.lu.se](mailto:karin.mattsson@biochemistry.lu.se)

### Author Contributions

The manuscript was written through contributions of all authors. All authors have given approval to the final version of the manuscript.

### Funding

The study was supported by grants from the Centre for Environmental and Climate Research, the Nanometer Structure Consortium at Lund University, and the Swedish Research Council.

### Notes

The authors declare no competing financial interest.

## ACKNOWLEDGMENTS

The authors thank Allan Lickander at Eslövs kommun for the permission to collect fish from lake Trollsjön, Niels Jepsen at Technical University of Denmark for thoughtful comments on the manuscript, Giuseppe Bianco for input on ImageJ code, and Filip Persson for input on MATLAB code.

## ABBREVIATIONS

CPMG	Carr–Purcell–Meiboom–Gill
DLS	dynamic light scattering
fwhm	full width at half maximum
HDL	high-density lipoprotein
MANOVA	multivariate analysis of variance
NMR	nuclear magnetic resonance
NTA	nanoparticle tracking analysis
PCA	principal component analysis
TOC	total organic carbon
TSP	trimethylsilyl propionate
UV	ultraviolet

## REFERENCES

- Rochman, C. M.; Browne, M. A. Classify plastic waste as hazardous. *Nature* **2013**, *494* (7436), 169–171.
- Cozar, A.; Echevarria, F.; Gonzalez-Gordillo, J. I.; Irigoien, X.; Ubeda, B.; Hernandez-Leon, S.; Palma, A. T.; Navarro, S.; Garcia-de-Lomas, J.; Ruiz, A.; Fernandez-de-Puelles, M. L.; Duarte, C. M. Plastic debris in the open ocean. *Proc. Natl. Acad. Sci. U.S.A.* **2014**, *111* (28), 10239–10244.
- Wegner, A.; Besseling, E.; Foekema, E. M.; Kamermans, P.; Koelmans, A. A. Effects of nanopolystyrene on the feeding behavior of the blue mussel (*Mytilus edulis* L.). *Environ. Toxicol. Chem.* **2012**, *31* (11), 2490–2497.
- Imhof, H. K.; Schmid, J.; Niessner, R.; Ivleva, N. P.; Laforsch, C. A novel, highly efficient method for the separation and quantification of plastic particles in sediments of aquatic environments. *Limnol. Oceanogr.: Methods* **2012**, *10*, 524–537.
- Gregory, M. R. Environmental implications of plastic debris in marine settings—Entanglement, ingestion, smothering, hangers-on, hitch-hiking, and alien invasions. *Philos. Trans. R. Soc. London, Ser. B* **2009**, *364* (1526), 2013–2025.
- Thompson, R.; Moore, C.; Andrady, A.; Gregory, M.; Takada, H.; Weisberg, S. New directions in plastic debris. *Science* **2005**, *310* (5751), 1117–1117.
- Thompson, R. C.; Olsen, Y.; Mitchell, R. P.; Davis, A.; Rowland, S. J.; John, A. W. G.; McGonigle, D.; Russell, A. E. Lost at sea: Where is all the plastic? *Science* **2004**, *304* (5672), 838–838.
- Nowack, B.; Bucheli, T. D. Occurrence, behavior, and effects of nanoparticles in the environment. *Environ. Pollut.* **2007**, *150* (1), 5–22.
- Zhu, H.; Han, J.; Xiao, J. Q.; Jin, Y. Uptake, translocation, and accumulation of manufactured iron oxide nanoparticles by pumpkin plants. *J. Environ. Monit.* **2008**, *10* (6), 713–717.
- Domingos, R. F.; Baalousha, M. A.; Ju-Nam, Y.; Reid, M. M.; Tufenkji, N.; Lead, J. R.; Leppard, G. G.; Wilkinson, K. J. Characterizing manufactured nanoparticles in the environment: Multimethod determination of particle sizes. *Environ. Sci. Technol.* **2009**, *43* (19), 7277–7284.
- Klaine, S. J.; Alvarez, P. J. J.; Batley, G. E.; Fernandes, T. F.; Handy, R. D.; Lyon, D. Y.; Mahendra, S.; McLaughlin, M. J.; Lead, J. R. Nanomaterials in the environment: Behavior, fate, bioavailability, and effects. *Environ. Toxicol. Chem.* **2008**, *27* (9), 1825–1851.
- Ferry, J. L.; Craig, P.; Hexel, C.; Sisco, P.; Frey, R.; Pennington, P. L.; Fulton, M. H.; Scott, I. G.; Decho, A. W.; Kashiwada, S.; Murphy, C. J.; Shaw, T. J. Transfer of gold nanoparticles from the water column to the estuarine food web. *Nat. Nanotechnol.* **2009**, *4* (7), 441–444.
- Moore, M. N. Do nanoparticles present ecotoxicological risks for the health of the aquatic environment? *Environ. Int.* **2006**, *32* (8), 967–976.
- Oberdorster, E. Manufactured nanomaterials (fullerenes, C60) induce oxidative stress in the brain of juvenile largemouth bass. *Environ. Health Perspect.* **2004**, *112* (10), 1058–62.
- Rosenkranz, P.; Chaudhry, Q.; Stone, V.; Fernandes, T. F. A comparison of nanoparticle and fine particle uptake by *Daphnia magna*. *Environ. Toxicol. Chem.* **2009**, *28* (10), 2142–2149.
- Wigginton, N. S.; Haus, K. L.; Hochella, M. F. Aquatic environmental nanoparticles. *J. Environ. Monit.* **2007**, *9* (12), 1306–1316.
- Gottschalk, F.; Sonderer, T.; Scholz, R. W.; Nowack, B. Modeled environmental concentrations of engineered nanomaterials (TiO<sub>2</sub>, ZnO, Ag, CNT, fullerenes) for different regions. *Environ. Sci. Technol.* **2009**, *43* (24), 9216–9222.
- Ytreberg, E.; Karlsson, J.; Ndungu, K.; Hasselov, M.; Breitbarth, E.; Eklund, B. Influence of salinity and organic matter on the toxicity of Cu to a brackish water and marine clone of the red macroalgae *Ceramium tenuicorne*. *Ecotoxicol. Environ. Saf.* **2011**, *74* (4), 636–642.
- Cedervall, T.; Lynch, I.; Lindman, S.; Berggard, T.; Thulin, E.; Nilsson, H.; Dawson, K. A.; Linse, S. Understanding the nanoparticle–protein corona using methods to quantify exchange rates and affinities of proteins for nanoparticles. *Proc. Natl. Acad. Sci. U.S.A.* **2007**, *104* (7), 2050–2055.
- Dell’Orco, D.; Lundqvist, M.; Oslakovic, C.; Cedervall, T.; Linse, S. Modeling the time evolution of the nanoparticle–protein corona in a body fluid. *PLoS One* **2010**, *5* (6), e10949.
- Tenzer, S.; Docter, D.; Kuharev, J.; Musyanovych, A.; Fetz, V.; Hecht, R.; Schlenk, F.; Fischer, D.; Kiouptsi, K.; Reinhardt, C.; Landfester, K.; Schild, H.; Maskos, M.; Knauer, S. K.; Stauber, R. H. Rapid formation of plasma protein corona critically affects nanoparticle pathophysiology. *Nat. Nanotechnol.* **2013**, *8* (10), 772–U1000.
- Lundqvist, M.; Stigler, J.; Elia, G.; Lynch, I.; Cedervall, T.; Dawson, K. A. Nanoparticle size and surface properties determine the protein corona with possible implications for biological impacts. *Proc. Natl. Acad. Sci. U.S.A.* **2008**, *105* (38), 14265–14270.
- Wang, F.; Yu, L.; Monopoli, M. P.; Sandin, P.; Mahon, E.; Salvati, A.; Dawson, K. A. The biomolecular corona is retained during nanoparticle uptake and protects the cells from the damage induced by cationic nanoparticles until degraded in the lysosomes. *Nanomedicine (N.Y., N.Y., U.S.)* **2013**, *9* (8), 1159–1168.
- Zhang, H.; Burnum, K. E.; Luna, M. L.; Petritis, B. O.; Kim, J. S.; Qian, W. J.; Moore, R. J.; Heredia-Langner, A.; Webb-Robertson, B. J.; Thrall, B. D.; Camp, D. G.; Smith, R. D.; Pounds, J. G.; Liu, T. Quantitative proteomics analysis of adsorbed plasma proteins classifies nanoparticles with different surface properties and size. *Proteomics* **2011**, *11* (23), 4569–4577.
- Cedervall, T.; Hansson, L. A.; Lard, M.; Frohm, B.; Linse, S. Food chain transport of nanoparticles affects behavior and fat metabolism. *PLoS One* **2012**, *7* (2), e32254.
- Hellstrand, E.; Lynch, I.; Andersson, A.; Drakenberg, T.; Dahlback, B.; Dawson, K. A.; Linse, S.; Cedervall, T. Complete high-density lipoproteins in nanoparticle corona. *FEBS J.* **2009**, *276* (12), 3372–3381.
- Cedervall, T.; Lynch, I.; Foy, M.; Berggard, T.; Donnelly, S. C.; Cagney, G.; Linse, S.; Dawson, K. A. Detailed identification of plasma proteins adsorbed on copolymer nanoparticles. *Angew. Chem., Int. Ed.* **2007**, *46* (30), 5754–5756.
- Tocher, D. R. Metabolism and functions of lipids and fatty acids in teleost fish. *Rev. Fish. Sci.* **2003**, *11* (2), 107–184.
- Andrady, A. L.; Neal, M. A. Applications and societal benefits of plastics. *Philos. Trans. R. Soc. London, Ser. B* **2009**, *364* (1526), 1977–1984.
- Moore, C. J. Synthetic polymers in the marine environment: A rapidly increasing, long-term threat. *Environ. Res.* **2008**, *108* (2), 131–139.
- Nicholson, J. K.; Lindon, J. C.; Holmes, E. ‘Metabonomics’: Understanding the metabolic responses of living systems to



pathophysiological stimuli via multivariate statistical analysis of biological NMR spectroscopic data. *Xenobiotica* **1999**, *29* (11), 1181–1189.

(32) Holm, S. A simple sequentially rejective multiple test procedure. *Scand. J. Stat.* **1979**, *6* (2), 65–70.

(33) Savorani, F.; Tomasi, G.; Engelsen, S. B. icoshift: A versatile tool for the rapid alignment of 1D NMR spectra. *J. Magn. Reson.* **2010**, *202* (2), 190–202.

(34) Trygg, J.; Wold, S. Orthogonal projections to latent structures (O-PLS). *J. Chemom.* **2002**, *16* (3), 119–128.

(35) Cui, Q.; Lewis, I. A.; Hegeman, A. D.; Anderson, M. E.; Li, J.; Schulte, C. F.; Westler, W. M.; Eghbalian, H. R.; Sussman, M. R.; Markley, J. L. Metabolite identification via the Madison Metabolomics Consortium Database. *Nat. Biotechnol.* **2008**, *26* (2), 162–164.

(36) Fan, W. M. T. Metabolite profiling by one- and two-dimensional NMR analysis of complex mixtures. *Prog. Nucl. Magn. Reson. Spectrosc.* **1996**, *28*, 161–219.

(37) Smith, C. J.; Shaw, B. J.; Handy, R. D. Toxicity of single walled carbon nanotubes to rainbow trout, (*Oncorhynchus mykiss*): Respiratory toxicity, organ pathologies, and other physiological effects. *Aquat. Toxicol.* **2007**, *82* (2), 94–109.

(38) Hansson, L. A.; Nicolle, A.; Graneli, W.; Hallgren, P.; Kritzberg, E.; Persson, A.; Bjork, J.; Nilsson, P. A.; Bronmark, C. Food-chain length alters community responses to global change in aquatic systems. *Nat. Clim. Change* **2013**, *3* (7436), 228–233.

(39) Kashiwada, S. Distribution of nanoparticles in the see-through medaka (*Oryzias latipes*). *Environ. Health Perspect.* **2006**, *114* (11), 1697–1702.

(40) Rossi, G.; Bamoud, J.; Monticelli, L. Polystyrene nanoparticles perturb lipid membranes. *J. Phys. Chem. Lett.* **2014**, *5* (1), 241–246.